# Gas-Particle Partitioning of Atmospheric Hg(II) and Its Effect on Global Mercury Deposition

Atmos. Chem. Phys., 12, 591–603, 2012
www.atmos-chem-phys.net/12/591/2012/
doi:10.5194/acp-12-591-2012


Atmospheric Chemistry and Physics

# Gas-particle partitioning of atmospheric Hg(II) and its effect on global mercury deposition

**H. M. Amos[1], D. J. Jacob[1,2], C. D. Holmes[3], J. A. Fisher[1], Q. Wang[2], R. M. Yantosca[2], E. S. Corbitt[1], E. Galarneau[4], A. P. Rutter[5], M. S. Gustin[6], A. Steffen[4], J. J. Schauer[7], J. A. Graydon[8], V. L. St. Louis[8], R. W. Talbot[9], E. S. Edgerton[10], Y. Zhang[11], and E. M. Sunderland[2,12]**

[1]Department of Earth and Planetary Sciences, Harvard University, Cambridge, MA, USA
[2]School of Engineering and Applied Sciences, Harvard University, Boston, MA, USA
[3]Department of Earth System Science, University of California, Irvine, CA, USA
[4]Air Quality Research Division, Environment Canada, Toronto, Ont., Canada
[5]Civil and Environmental Engineering Department, Rice University, Houston, TX, USA
[6]Department of Natural Resources and Environmental Sciences, University of Nevada, Reno, NV, USA
[7]Department of Civil and Environmental Engineering, University of Wisconsin, Madison, WI, USA
[8]Department of Biological Sciences, University of Alberta, Edmonton, Alberta, Canada
[9]Department of Earth and Atmospheric Sciences, University of Houston, Houston, TX, USA
[10]Atmospheric Research & Analysis, Inc., Cary, NC, USA
[11]Department of Atmospheric Sciences, University of Washington, Seattle, USA
[12]Department of Environmental Health, Harvard University, Boston, MA, USA

*Correspondence to:* H. M. Amos (amos@fas.harvard.edu)

Received: 19 October 2011 – Published in Atmos. Chem. Phys. Discuss.: 31 October 2011
Revised: 30 December 2011 – Accepted: 2 January 2012 – Published: 11 January 2012

**Abstract.** Atmospheric deposition of Hg(II) represents a major input of mercury to surface environments. The phase of Hg(II) (gas or particle) has important implications for deposition. We use long-term observations of reactive gaseous mercury (RGM, the gaseous component of Hg(II)), particle-bound mercury (PBM, the particulate component of Hg(II)), fine particulate matter ($PM_{2.5}$), and temperature ($T$) at five sites in North America to derive an empirical gas-particle partitioning relationship $\log_{10}(K^{-1}) = (10\pm1)–(2500\pm300)/T$ where $K = (PBM/PM_{2.5})/RGM$ with PBM and RGM in common mixing ratio units, $PM_{2.5}$ in $\mu g\,m^{-3}$, and $T$ in K. This relationship is within the range of previous work but is based on far more extensive data from multiple sites. We implement this empirical relationship in the GEOS-Chem global 3-D Hg model to partition Hg(II) between the gas and particle phases. The resulting gas-phase fraction of Hg(II) ranges from over 90 % in warm air with little aerosol to less than 10 % in cold air with high aerosol. Hg deposition to high latitudes increases because of more efficient scavenging of particulate Hg(II) by precipitating snow. Model comparison to Hg observations at the North American surface sites suggests that subsidence from the free troposphere (warm air, low aerosol) is a major factor driving the seasonality of RGM, while elevated PBM is mostly associated with high aerosol loads. Simulation of RGM and PBM at these sites is improved by including fast in-plume reduction of Hg(II) emitted from coal combustion and by assuming that anthropogenic particulate Hg(p) behaves as semivolatile Hg(II) rather than as a refractory particulate component. We improve the simulation of Hg wet deposition fluxes in the US relative to a previous version of GEOS-Chem; this largely reflects independent improvement of the washout algorithm. The observed wintertime minimum in wet deposition fluxes is attributed to inefficient snow scavenging of gas-phase Hg(II).

## 1 Introduction

Mercury (Hg) is a naturally occurring metal that can cause adverse health effects in humans and wildlife (Clarkson and Magos, 2006; Mergler et al., 2007; Scheuhammer et al.,

**Table 1.** Measurement sites for RGM and PBM.

| Site | Location | Record | $PM_{2.5}$ data[a] | Reference |
|---|---|---|---|---|
| Experimental Lakes Area, Ontario | 49.7° N, 93.7° W | May 2005–Dec 2009 | [b] | Graydon et al. (2008) |
| Milwaukee, Wisconsin | 43.1° N, 87.8° W | Jul 2004–May 2005 | [c] | Rutter and Schauer (2007b) |
| Outlying Landing Field (Pensacola), Florida | 30.6° N, 87.4° W | Jan 2009–Dec 2009 | [c] | Edgerton et al. (2006) |
| Reno, Nevada | 39.3° N, 119.5° W | Feb 2007–Jan 2009 | [d] | Lyman and Gustin (2009) |
| Thompson Farm, New Hampshire | 43.1° N, 71.0° W | Jan 2009–Jun 2010 | [d] | Sigler et al. (2009) |

[a] All $PM_{2.5}$ data are 24-h averages. [b] $PM_{2.5}$ from nearby Voyageurs National Park IMPROVE site (http://vista.cira.colostate.edu/IMPROVE/).
[c] $PM_{2.5}$ collocated with Hg measurements. [d] $PM_{2.5}$ from a nearby EPA Air Quality System site (http://www.epa.gov/ttn/airs/airsaqs).

2007). Human exposure in developed countries is mainly through consumption of contaminated fish (Mahaffey et al., 2004; 2009). As a result of anthropogenic emissions, deposition to the oceans has increased roughly threefold since the pre-industrial era (Mason and Sheu, 2002; Sunderland and Mason, 2007). Mercury is released to the atmosphere mainly as elemental mercury (Hg(0)), though combustion processes also emit divalent mercury (Hg(II)). Hg(0) in the atmosphere can eventually be oxidized to Hg(II). Hg(II) compounds have low vapor pressure ($HgCl_2$ $8.99\times10^{-3}$ Pa at 20 °C, HgO $9.20\times10^{-12}$ Pa at 25 °C), and thus partition between the gas and particle phases and are removed by wet and dry deposition (Schroeder and Munthe, 1998; Lin et al., 2006). The phase partitioning of Hg(II) has important implications for deposition because gases and particles are deposited by different physical processes and at different rates (Seinfeld and Pandis, 2006). Hg(0) has a high vapor pressure (0.18 Pa at 20 °C, Schroeder and Munthe, 1998) so that its sorption to particles is thought to be generally negligible (Seigneur et al., 1998). Here we use long-term observational records of speciated atmospheric Hg to develop a mechanistic parameterization of Hg(II) gas-particle partitioning and apply it to a simulation of Hg deposition in the GEOS-Chem global 3-D chemical transport model (CTM).

There is considerable uncertainty regarding the atmospheric redox chemistry of Hg (Hynes et al., 2009), and atmospheric measurement methods are subject to artifacts (Gustin and Jaffe, 2010). Current measurements use an operationally defined method for quantifying reactive gaseous mercury (RGM) and fine fraction (<2.5 µm) particle-bound mercury (PBM) (Lamborg et al., 1995; Keeler et al., 1995; Landis et al., 2002). Rutter and Schauer (2007b) investigated the mechanism of Hg partitioning in air by fitting urban and laboratory data for RGM and PBM to a temperature-dependent expression for Hg(II) sorption onto PM smaller than 2.5 µm in diameter ($PM_{2.5}$). This approach is similar to parameterizations previously developed for other semi-volatile species including polycyclic aromatic hydrocarbons (Yamasaki et al., 1982; Pankow, 1987) and secondary organic compounds (Pankow, 1994; Odum et al., 1996; Chung and Seinfeld, 2002).

Little was known about Hg(II) gas-particle partitioning prior to the work of Rutter and Schauer et al. (2007a, b). Earlier models of atmospheric Hg included parameterizations for the sorption of dissolved Hg species to soot particles suspended in cloud water (Petersen et al., 1998; Seigneur et al., 2001; Bullock and Brehme, 2002; Dastoor and Larocque, 2004) based on experimental results from Petersen et al. (1995) and Seigneur et al. (1998). In more recent years, models of atmospheric Hg have taken various approaches to treating Hg(II) gas-particle partitioning. Vijayaraghavan et al. (2008) implemented the temperature-dependent Hg(II) gas-particle partitioning formulation of Rutter and Schauer (2007b) into a regional model for the United States. Previous versions of GEOS-Chem have either assumed atmospheric Hg(II) to be entirely gas-phase (Selin et al., 2007, 2008) or 50/50 gas/particle (Holmes et al., 2010).

Here we use long-term RGM and PBM observations at five sites in North America to derive an empirical gas-particle Hg(II) partitioning coefficient as a function of $PM_{2.5}$ and temperature, following the approach of Rutter and Schauer (2007b) but with a much larger data set. We show that a single parameterization can describe the Hg(II) partitioning across sites, and compare the resulting GEOS-Chem simulation to observations. The implications for global Hg deposition are discussed.

## 2 Hg(II) gas-particle partitioning

RGM and PBM data were obtained from five sites: Reno, Nevada; Thompson Farm, New Hampshire; Outlying Landing Field (Pensacola), Florida; Experimental Lakes Area, Ontario; and Milwaukee, Wisconsin (Table 1). The Experimental Lakes site includes 4 years of data, the Reno site 2 years, and the others one year or slightly less. Figures 1 and 2 show the spatial and seasonal distributions of the data and are discussed in Sect. 4.

All Hg measurements were collected with Tekran mercury analyzers (2537A, 1130, and 1135 units). Air is drawn through a heated (50 °C) impactor which removes coarse (>2.5 µm) particles from the air stream, then through a

**Table 2.** Regression coefficients for $\log_{10}(K^{-1}) = a + b/T$.

| Site[a] | $a$ | $b$ | $r^2$ | Reference |
|---|---|---|---|---|
| Experimental Lakes | 9±4 | −2400±1100 | 0.57 | this work |
| Milwaukee | 7±2 | −1900±400 | 0.43 | this work |
| Pensacola | 6±2 | −1600±600 | 0.16 | this work |
| Reno | 13±2 | −3300±600 | 0.54 | this work |
| Thompson Farm | 8±6 | −2000±1600 | 0.33 | this work |
| All sites above (combined) | 10±1 | −2500±300 | 0.49 | this work |
| Urban[b,c] | 15±2 | −4250±480 | 0.77 | Rutter and Schauer (2007b) |
| Urban[d] | 7±1 | −1710±380 | 0.49 | Rutter and Schauer (2007b) |
| Laboratory, $HgCl_2$ on $(NH_4)_2SO_4$[e] | 19±2 | −5720±470 | 0.99 | Rutter and Schauer (2007b) |
| Laboratory, $HgCl_2$ on adipic acid[e] | 9±1 | −2780±240 | 0.96 | Rutter and Schauer (2007b) |

[a] Measurements of RGM and PBM were made by Tekran instruments unless otherwise indicated. [b] Hg collected using filter-based methods (Rutter and Schauer, 2007a, b). [c] Milwaukee (July 2004–May 2005) and Riverside, California (16 July–7 August 2005), Rutter and Schauer (2007b). [d] Milwaukee (July 2004–May 2005) (Rutter and Schauer, 2007b). [e] Dry conditions (RH < 1 %).

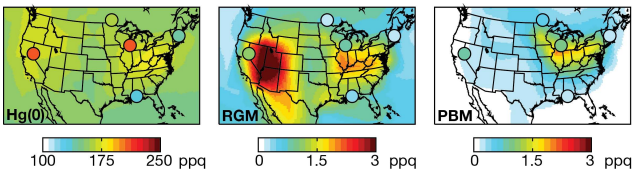


**Fig. 1.** Simulated (background solid contours) and observed (circles) annual mean concentrations of speciated Hg. Measurement sites and measurement periods are listed in Table 1. Model results are for 2007–2009.

KCl-coated annual denuder to collect RGM, followed by a quartz fiber filter to collect PBM (Landis et al., 2002). The filter and denuder are sequentially heated to 800 °C and 500 °C, respectively, to thermally desorb the collected RGM and PBM. The desorbed RGM and PBM are sequentially reduced to Hg(0) as they pass through an 800 °C pyrolyzer and are finally analyzed as Hg(0) by cold vapor atomic fluorescence spectroscopy (CVAFS). Previous work has suggested that there are artifacts associated with PBM collection (Lynam and Keeler, 2005; Malcolm and Keeler, 2007; Rutter et al., 2008a; Talbot et al., 2011) and interferences with the collection of RGM on KCl coated denuders (Lyman et al., 2010).

Keeping the limitations of the Tekran instrument in mind, we use them in the absence of other information. We parameterize the partitioning of Hg(II) between the gas and particle phases with a partitioning coefficient $K$ (Rutter and Schauer, 2007a, b):

$$K = (\mathrm{PBM}/\mathrm{PM}_{2.5})/\mathrm{RGM} \quad (1)$$

where RGM and PBM are atmospheric mixing ratios (ppq) and $PM_{2.5}$ is the dry mass concentration ($\mu g\,m^{-3}$). It is assumed that Eq. (1) represents equilibrium between the gas and particle phases of atmospheric Hg(II), and that the major Hg(II) compounds measured as RGM and PBM have similar volatilities so that a single equilibrium constant is applicable. Normalization by $PM_{2.5}$ makes the additional assumption that uptake is proportional to the aerosol mass concentration, although adsorption to a solid aerosol phase would be equivalent if a fixed scaling is assumed between the volume and area of the aerosol (Yamasaki et al., 1982; Pankow, 1987; Rutter and Schauer, 2007a, b). Restriction to fine aerosol ($PM_{2.5}$) in Eq. (1) is consistent with the size cut-off of the Tekran instrument.

Previous applications of Eq. (1) to polycyclic aromatic hydrocarbons and secondary organic aerosol found a van't Hoff type of relationship between $K$ and the local temperature $T$ (Yamasaki et al., 1982; Pankow, 1987):

$$\log_{10}(K^{-1}) = a + \frac{b}{T} \quad (2)$$

where $a$ and $b$ are coefficients. Figure 3 shows the daily data from the sites in Table 1 fit to Eq. (2). Confidence intervals (95 %) for the slope and intercept are constructed using a bootstrap method. All RGM and PBM observations are averaged over midday hours (10:00–16:00 local time) when vertical mixing is strongest and the air mass being sampled is more likely to be homogenous. $PM_{2.5}$ data are 24-h averages as no higher temporal resolution is available. Use of 24-h average RGM and PBM data, as compared to daytime averages, does not significantly change our results. Pankow et al. (1993) suggested that relative humidity (RH) affects gas-particle partitioning of semi-volatile organic compounds. We tested this for Hg by performing a multivariate regression, $\log_{10}(K^{-1}) = a + b/T + c\mathrm{RH}$, and found no significant dependence on RH at any of the sites.

Table 2 lists the regression fits for individual sites. We tested them for statistical distinctness following Galarneau et al. (2006). Reno, Thompson Farm, and Experimental Lakes are statistically indistinct, as are Milwaukee, Pensacola,

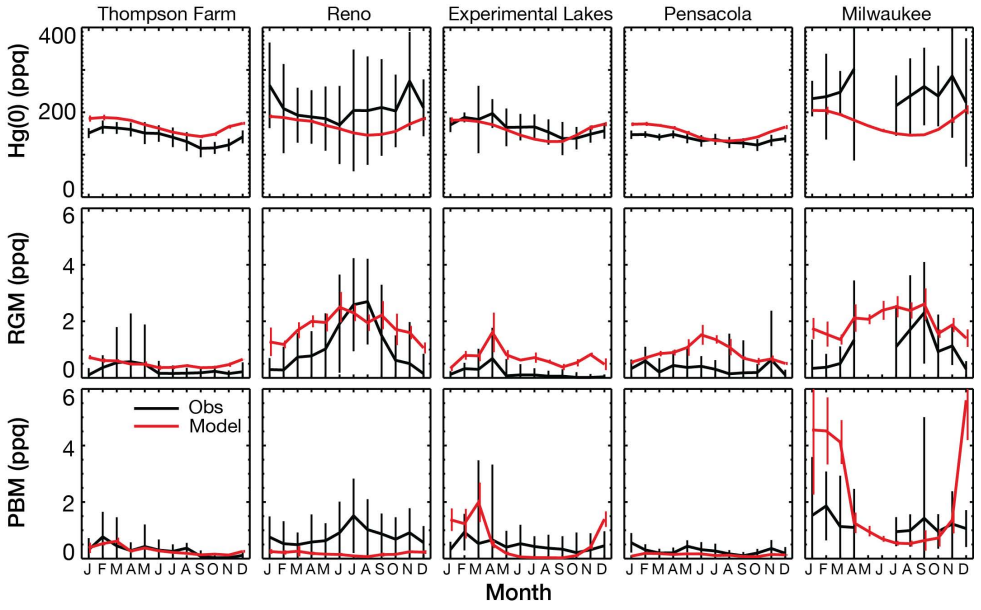


**Fig. 2.** Monthly mean observed (black, $\pm 1\sigma$) and simulated (red, $\pm 1\sigma$) concentrations of speciated Hg during daytime hours (10:00–16:00 local time). Standard deviations for simulated Hg(0) are less than the width of the line. Measurement sites and measurement periods are listed in Table 1. Each month contain at least two weeks of daily measurements. Model results are for 2007–2009.

Thompson Farm, and Experimental Lakes. Reno is distinct from Pensacola and Milwaukee. Differences in aerosol composition between sites would be expected to affect the fits (Rutter and Schauer, 2007a, b) but we do not have composition information to pair with the mercury observations. We investigated seasonal variations in the fits for individual sites but found that the resulting correlations were not robust because of insufficient number of data points and insufficient dynamic range in temperature. The regression fit for the combined data set (all sites) is $\log(K^{-1}) = (10 \pm 1) - (2500 \pm 300)/T$ ($r^2 = 0.49$) and will be used in the analysis below. It is statistically indistinct from the individual regressions for each site except Reno.

Our regression fit for the combined data falls between those reported by Rutter and Schauer (2007b) for urban measurements using a filter-based method and a Tekran instrument (Fig. 3). Our fit is statistically indistinct from their laboratory data for partitioning of $HgCl_2$ with adipic acid aerosol and differs most from their partitioning of $HgCl_2$ to dry, synthesized $(NH_4)_2SO_4$ aerosol (Table 2). Rutter and Schauer (2007b) hypothesized that the difference in partitioning between their filter-based method and the Tekran instrument could reflect a sampling artifact associated with internally heating the Tekran instrument to 50 °C. Comparison of our regression with the filter-based regression of Rutter and Schauer (2007b) in Fig. 3 would imply a ∼30 °C thermal bias, although the filter-based regression is based on very limited data. We will discuss the effect of the possible thermal bias in the GEOS-Chem simulation of Hg atmospheric concentrations and wet deposition fluxes.

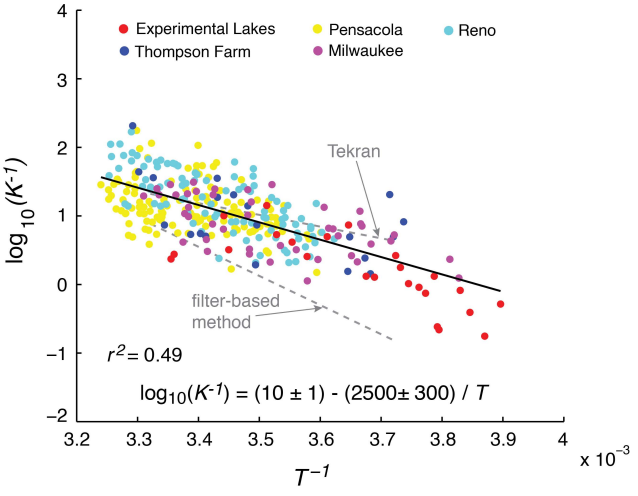


**Fig. 3.** Temperature dependence of the relationship between gas-phase and particle-phase Hg as defined by Eqs. (1) and (2). Each point represents one observation day (10:00–16:00 local time) for the color-coded sites in Table 1. Days with RGM or PBM below 0.34 ppq, or $PM_{2.5}$ below 2 µg $m^{-3}$, are rejected as below analytical detection limits. Temperature is in K. Also shown is the least-squares regression line for the ensemble of points (solid) and the regression parameters with 95 % bootstrapped confidence intervals. Shown in dashed grey are the least-squares regression lines from Rutter and Schauer (2007b) for urban data collected using a filter-based method and a Tekran instrument.

## 3 GEOS-chem model simulation

We use version 9-01-01 of the GEOS-Chem Hg coupled atmosphere-ocean-land model (www.geos-chem.org), which includes an atmosphere from Holmes et al. (2010), a surface ocean from Soerensen et al. (2010), and a land surface from Selin et al. (2008). The simulation is conducted for 2004-2009 with GEOS-5 assimilated meteorological and surface data from the NASA Global Modeling and Assimilation Office (GMAO). The years 2004–2006 are used for initialization and 2007–2009 for analysis. The original GEOS-5 data have $1/2^\circ \times 2/3^\circ$ horizontal resolution and 72 vertical levels. The horizontal resolution is degraded here to $4^\circ \times 5^\circ$ for input to GEOS-Chem. The GEOS-Chem simulation transports two Hg tracers in the atmosphere: elemental Hg (Hg(0)) and divalent Hg (Hg(II)). Atmospheric Hg(0)/Hg(II) redox chemistry follows Holmes et al. (2010), with oxidation of Hg(0) by Br atoms and photoreduction of Hg(II) in liquid cloud droplets. Oxidation of Hg(0) by $OH/O_3$ is an alternative to oxidation by Br in GEOS-Chem (Holmes et al., 2010), but we do not use the $OH/O_3$ reaction scheme (Hall, 1995; Sommar et al., 2001) here because of doubt in the associated kinetics (Calvert and Lindberg, 2005; Hynes et al., 2009; Subir et al., 2011). Hg(II) is assumed to be in equilibrium between the gas and particle phases at all times. Earlier versions of GEOS-Chem included a separate particulate Hg(p) tracer emitted by combustion and assumed to be inert, but here we assume that Hg(p) is emitted as Hg(II) and merge it with the Hg(II) tracer. This greatly improves the model simulation of PBM at surface sites, as discussed in Sect. 4.

Direct emission of Hg(II) in GEOS-Chem is entirely anthropogenic, while Hg(0) is emitted from both natural and anthropogenic sources (Schroeder and Munthe, 1998). Anthropogenic emissions are from the Pacyna et al. (2010) inventory for the year 2005 and are speciated in that inventory as Hg(0), Hg(II), and Hg(p) (which we emit as Hg(II)). Fossil fuel combustion accounts for 46 % of the global anthropogenic source in the Pacyna et al. (2010) inventory with a Hg(0):Hg(II):Hg(p) speciation of 50:40:10. However, observations in power plant plumes by Edgerton et al. (2006) indicate that Hg(0) accounts on average for 84 % of total Hg, much higher than implied by the emission inventory. Similarly, measurements downwind of power plants by Weiss-Penzias et al. (2011) suggest that the average RGM fraction (21 % and 8 % at two different sites) is much lower than estimated by the local NEI 2002 emission inventory (∼58 %). Dirigible measurements by ter Schure et al. (2011) suggest that the discrepancy does not reflect errors in the emission inventories but instead rapid in-plume reduction operating by a mechanism not found in the background atmosphere.

Several model studies also provide support for in-plume reduction of Hg(II) emitted from power plants (Seigneur et al., 2003; Lohman et al., 2006; Seigneur et al., 2006; Vijayaraghavan et al., 2008; Kos et al., 2011; Y. Zhang et al., 2011). Y. Zhang et al. (2011) use a 86.5:9.9:3.6 (Hg(0):Hg(II):Hg(p)) speciation for fossil fuel combustion in a nested version of GEOS-Chem over North America and demonstrate significantly improved comparison to surface Hg observations and Hg wet deposition fluxes from the Mercury Deposition Network (MDN). Kos et al. (2011) implemented a 90:8:2 speciation in the GRAHM global model to better match surface concentrations of RGM and PBM over North America. Here we follow the emission speciation of Y. Zhang et al. (2011), which is consistent with the above studies and greatly reduces the model bias compared to observations of RGM and PBM (see Sect. 4). This implicit inclusion of Hg(II) in-plume reduction in the model comes with the important caveats that a chemical mechanism has not been indentified (Lohman et al., 2006) and that there are significant uncertainties associated with both the speciation of anthropogenic emission inventories (AMAP/UNEP, 2008) and the methods for measuring atmospheric Hg (Gustin and Jaffe, 2010).

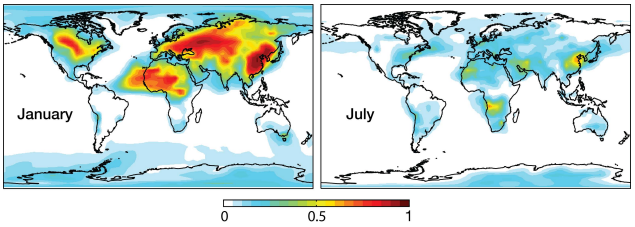


**Fig. 4.** Mean fraction of Hg(II) partitioned into the particle phase in surface air in January and July. Values are 2007–2009 GEOS-Chem model results obtained using Eqs. (1) and (2), not including partitioning into sea-salt aerosol which is treated separately following Holmes et al. (2010).

Partitioning of Hg(II) between the gas and particle phases in GEOS-Chem is computed using local GEOS-5 temperature and archived monthly mean 3-D $PM_{2.5}$ from a detailed GEOS-Chem aerosol simulation for the year 2007 (L. Zhang et al., 2011a). $PM_{2.5}$ is specified as the sum of sulfate, nitrate, ammonium, carbonaceous, and fine dust particle mass. The resulting Hg(II) particulate fraction in the model ranges from less than 10 % in warm environments with low aerosol to more than 90 % in cold environments with high aerosol (Fig. 4). Gas-particle partitioning of Hg(II) with sea-salt particles in the marine boundary layer is accounted for separately in GEOS-Chem as described by Holmes et al. (2009, 2010), using a physical model for uptake of Hg(II) by sea-salt aerosol based on formation of Hg-Cl complexes (Clever et al., 1985; Hedgecock and Pirrone, 2001).

Dry deposition in GEOS-Chem is computed with a standard resistance-in-series scheme and is much faster for water-soluble gases than for particles (Wesely, 1989). RGM has been observed to have very high dry deposition velocities (0.4–7.6 $cm\,s^{-1}$) (Lindberg and Stratton, 1998; Poissant et al., 2004; Skov et al., 2006; Lyman et al., 2007; Lyman et al., 2009) and so a negligibly small surface resistance is

assumed for gaseous Hg(II) (Selin et al., 2007). Dry deposition of particulate Hg(II) follows the standard surface resistance formulation of Wesely (1989) as implemented by Wang et al. (1998). Global annual mean dry deposition velocities in GEOS-Chem are 0.93 cm $s^{-1}$ for gaseous Hg(II) and 0.11 cm $s^{-1}$ for particulate Hg(II).

Wet deposition of Hg(II) in GEOS-Chem includes scavenging from moist convective updrafts as well as rainout and washout by large-scale precipitation (Liu et al., 2001; Holmes et al., 2010). Gaseous Hg(II) is scavenged as $HgCl_2$ with a Henry's law constant of $1.4\times10^6$ M $atm^{-1}$ (Lindqvist and Rodhe, 1985). We include recent GEOS-Chem improvements by Wang et al. (2011), which allow rainout and washout to occur in the same grid box and differentiate between aerosol scavenging by snow and rain. Both gaseous Hg(II) and particulate Hg(II) are retained by supercooled water during freezing (Holmes et al., 2010). There is observational evidence that falling snow is inefficient at scavenging RGM (Keeler et al., 2005; Sigler et al., 2009; Lombard et al., 2011; Mao et al., 2011) and so we do not allow below-cloud scavenging of gaseous Hg(II) by snow. We conducted a $^{222}$Rn-$^{210}$Pb simulation (Liu et al., 2001) to test the model representation of aerosol deposition. $^{210}$Pb is produced by decay of terrigenic $^{222}$Rn and attaches indiscriminately to aerosols, which are then removed by wet and dry deposition. We obtained a lifetime of tropospheric $^{210}$Pb against deposition of 10.4 days, consistent with a value of about 9 days in previous global 3-D model studies supported by comparisons to $^{222}$Rn and $^{210}$Pb observations (Balkanski et al., 1993; Koch et al., 1996; Liu et al., 2001).

An important update in this study is to correct an error in the washout of gases by rain in GEOS-Chem affecting the scavenging of highly soluble gases other than $HNO_3$ (and including gaseous Hg(II)). The GEOS-Chem washout scheme for gases had not been documented previously in the literature and we do so here (see Appendix), including the correction. After the correction we find that the global lifetime of tropospheric gaseous Hg(II) against wet deposition is reduced from 104 days to 46 days (the lifetime is relatively long because of the large fraction of the inventory in the upper troposphere).

We discussed above the tentative evidence for fast reduction of Hg(II) in power plant plumes. No such constraints are available for Hg(II) reduction in the background atmosphere. In models, Hg(II) reduction is generally assumed to take place by aqueous-phase photochemistry in clouds but is virtually unconstrained, with laboratory data for reduction rate constants spanning several orders of magnitude (Subir et al., 2011 and references therein). Past GEOS-Chem model studies have used Hg(II) reduction as a tuning parameter to reconcile emissions (natural and anthropogenic) with atmospheric Hg(0) concentrations (Selin et al., 2007), and similar tuning has been used in other models as well (Seigneur et al., 2006; Pongprueksa et al., 2008). Here we use an in-cloud reduction rate constant decreased by 50 % from that in Holmes et al. (2010), yielding a tropospheric Hg(II) lifetime of 2.4 months against reduction as compared to 1.7 months in Holmes et al. (2010).

We evaluated the model against the same global set of land and cruise ship Hg(0) measurements used by Holmes et al. (2010) and our results are similar (not shown here). Our global budget of Hg is similar to those in Holmes et al. (2010) and Soerensen et al. (2010). Global tropospheric burdens are 3600 Mg Hg(0) and 500 Mg Hg(II) (310 Mg gas and 190 Mg particulate). Net Hg(0) ocean evasion is 2900 Mg $a^{-1}$ (14 Mmol $a^{-1}$), which is consistent with Soerensen et al. (2010) and within the 90 % confidence intervals of 10–21 Mmol $a^{-1}$ simulated by Sunderland and Mason (2007). On a global scale, dry deposition is 2500 Mg $a^{-1}$ (55 % Hg(0) (land only), 45 % Hg(II)), wet deposition is 3000 Mg $a^{-1}$, and deposition of Hg(II) via sea salt is 1600 Mg $a^{-1}$.

## 4 Comparison to surface observations

Simulated annual mean Hg(0), RGM, and PBM concentrations are shown in Fig. 1. The correlation coefficients between the model and observations are $r_{Hg(0)} = 0.75$, $r_{RGM} = 0.93$, $r_{PBM} = 0.75$, which suggests that the model has some skill in simulating the spatial distribution of Hg species. The normalized mean biases (NMB) of the model are -5 %, 117 %, and 18 % for Hg(0), RGM, and PBM, respectively. Adjusting the anthropogenic emissions to account for in-plume reduction greatly improves the model. Without in-plume reduction of Hg(II) the NMB values would be 210 % for RGM and 96 % for PBM, with $r_{RGM} = 0.81$ and $r_{PBM} = 0.76$. We performed a sensitivity simulation using Rutter and Schauer's (2007b) gas-particle partitioning relationship derived from their filter-based method (Fig. 3, Table 2) to test the effect of a potential Tekran heating artifact. This yields $r_{RGM} = 0.92$ and $r_{PBM} = 0.79$, with NMBs of 11 %, and 237 % for RGM and PBM, respectively. PBM in that simulation is greatly overestimated.

RGM in the model is maximum over the western US where warm air with low aerosol subsides from the free troposphere (Selin and Jacob, 2008). PBM is maximum over the Midwest and eastern US where $PM_{2.5}$ concentrations and anthropogenic Hg emissions are high. An important aspect of our PBM simulation is the assumption that anthropogenic Hg(p) in emission inventories is emitted as Hg(II) and thus available for gas-particle partitioning and reduction. If we viewed instead Hg(p) as a refractory fine aerosol, as in previous versions of GEOS-Chem, the NMB for PBM at the five sites would increase to 100 %. Even though a refractory Hg(p) is inconsequential for the global Hg budget in the model (Holmes et al., 2010), it has a significant effect on surface air concentrations in source regions.

Simulated and observed monthly mean mixing ratios of Hg(0), RGM, and PBM are compared in Fig. 2. The NMB

of the model is −4 %, 117 %, and 18 % for Hg(0), RGM, and PBM, respectively with $r_{Hg(0)} = 0.39$, $r_{RGM} = 0.70$, and $r_{PBM} = 0.56$. The observed seasonality of Hg(0) at Thompson Farm, Experimental Lakes Area, and Pensacola is typical of northern mid-latitudes, with maximum in early spring and minimum in late summer/early fall. Photochemical destruction is thought to be the major process contributing to the summer decrease (Bergan and Rodhe, 2001; Selin et al., 2007; Holmes et al., 2010). The concentration of Hg(0) at Reno and Milwaukee is much greater and more variable, likely reflecting local urban sources (Rutter et al., 2008b; Lyman and Gustin, 2009) that are not resolved by the coarse horizontal resolution of the model.

There is much greater spatial variability for observed RGM and PBM than for Hg(0), reflecting the shorter lifetimes. An implication is that variability in RGM and PBM is not significantly driven by variability in Hg(0). Engle et al. (2010) previously examined the seasonality of speciated Hg at nine sites across central and eastern North America, and reported large site-to-site variability that they attributed to a complex combination of processes including local point sources, exchange between the boundary layer and the free troposphere, and coastal effects. Temperature and aerosol concentrations also play an important role through the partitioning between RGM and PBM.

RGM concentrations are highest at Reno and Milwaukee in summer, both in the observations and in the model. The summer maximum at Reno is due to entrainment of RGM-rich free tropospheric air during deep diurnal mixed layer growth (Lyman and Gustin, 2009; Weiss-Penzias et al., 2009). This entrainment is associated with low aerosol concentrations and high temperatures, so that there is little associated enhancement of PBM. Lyman and Gustin (2009) suggest that the observed summer peak in PBM at Reno is due to extensive wildfire plumes during the summer of 2008 affecting the area (Arnott et al., 2008), and this is consistent with other observations of enhanced PBM during wildfires (Friedli et al., 2003a, b; Finley et al., 2009). The elevated summer RGM at Milwaukee is due to regional anthropogenic sources in the Midwest (Rutter et al., 2008b), with a corresponding enhancement of PBM in winter when low temperatures cause this anthropogenic Hg(II) to be partitioned into the aerosol. The high model PBM at Milwaukee in winter is due to a local overestimate of ammonium nitrate aerosol in GEOS-Chem, thought to be caused by excessive $N_2O_5$ hydrolysis (L. Zhang et al., 2011b).

RGM and PBM at Thompson Farm and Experimental Lakes Area peak in winter-spring, both in the observations and in the model. In the model, this seasonality is due to subsidence of Hg(II)-rich air from the upper troposphere and lower stratosphere (UT/LS). Observational evidence suggests that the UT/LS contains a large reservoir of Hg(II) (Swartzendruber et al., 2006; Faïn et al., 2009). A parallel can be drawn to aerosol $^7$Be, which is cosmogenically produced in the UT/LS and removed by deposition; similar to RGM, observations and models of $^7$Be at northern mid-latitudes also show a winter-spring maximum (Liu et al., 2001; Yoshimori, 2005; Muramatsu et al., 2008; Alegría et al., 2010). At Pensacola, the spurious summer peak of RGM in the model appears to be due to excessively deep boundary layer mixing. That site is affected by sea breezes, which are not resolved by the model and would restrict boundary layer growth.

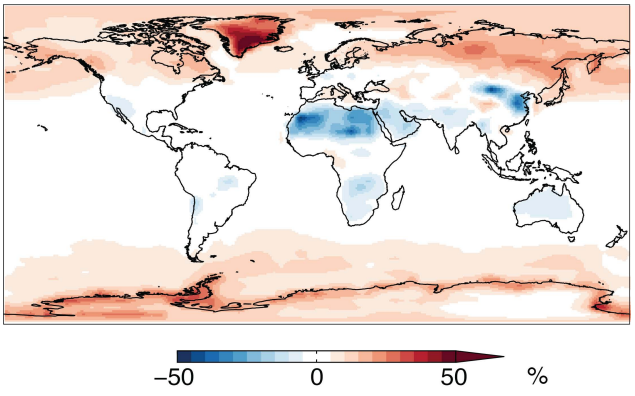


**Fig. 5.** Percent difference in total annual Hg(II) deposition between our standard simulation and a simulation where all Hg(II) is assumed to deposit as gas except for uptake by sea salt. Positive values indicate higher deposition in the standard simulation.

## 5 Implications for Hg deposition

Gas-particle partitioning impacts the global spatial distribution of Hg(II) deposition in the model. Figure 5 shows the relative difference in total Hg(II) deposition between our standard simulation and a sensitivity simulation where all Hg(II) is deposited as a gas except for uptake by sea salt. Partitioning Hg(II) into the aerosol in our standard simulation increases deposition at high latitudes because particulate Hg(II) is scavenged by precipitating snow but gaseous Hg(II) is not. By contrast, it decreases deposition over dry subtropical regions because gaseous Hg(II) is efficiently dry deposited but particulate Hg(II) is not. The effect over tropical and subtropical oceans is small because there is little non-sea-salt aerosol and so Hg(II) is either in the gas phase or in the sea-salt aerosol (which is treated the same in the two simulations).

The extensive MDN (2011) wet deposition flux data in the US have been used in previous GEOS-Chem studies to evaluate the model deposition (Selin et al., 2007, 2008; Selin and Jacob, 2008; Holmes et al., 2010). Uncertainty in the MDN measurements is 10–25 % (Gustin and Jaffe, 2010). Figure 6 compares model results to the MDN observed annual Hg wet deposition fluxes for 2007–2009. The NMB of the model is −11 % and the correlation coefficient is $r = 0.71$.

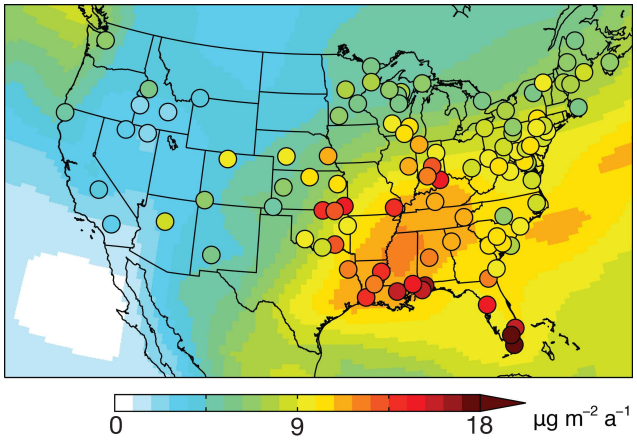


**Fig. 6.** Annual Hg wet deposition fluxes for 2007–2009. Model results (solid contours) are compared to measurements (circles) from the Mercury Deposition Network (MDN). The MDN observations have been averaged as in Holmes et al. (2010).

A sensitivity simulation using the filter-based Hg(II) gas-particle partitioning relationship from Rutter and Schauer (2007b) yields a NMB of 6.9 % and $r = 0.62$. The model captures the observed regional maximum in the Southeast US though not the particularly high values along the Gulf Coast. Y. Zhang et al. (2011) show that a nested GEOS-Chem simulation with $1/2° \times 2/3°$ horizontal resolution over North America has more skill at capturing these high values, perhaps due to better representation of deep convection. Our simulation improves over the previous GEOS-Chem version of Holmes et al. (2010) using Br as Hg(0) oxidant where the simulated eastern US maximum of Hg deposition was too far north. This largely reflects improvement of the washout algorithm (see Appendix and Wang et al. (2011)).

Selin and Jacob (2008) pointed out that the dominant modes of variability in the MDN data over the eastern US are a latitudinal gradient and a seasonal variation that decreases in amplitude with increasing latitude. Figure 7 compares observed and simulated seasonal variations of Hg wet deposition over the eastern US as a function of latitude, for the standard simulation and for sensitivity simulations with Hg(II) depositing either entirely as a gas or entirely as particles. For the standard simulation, $r = 0.85$ and the NMB of the model is $-11$ %. The standard model is able to capture the observed seasonal patterns of wet deposition and, except over the Gulf of Mexico, their latitude-dependent amplitudes. The sensitivity simulation with all Hg(II) depositing as particles and thus scavenged by snow shows significant overestimate of wet deposition in winter. This lends support to the notion that gaseous Hg(II) (∼50 % of total Hg(II) over US in winter, see Fig. 4) is not efficiently scavenged by snow. However, questions remain as to the MDN collection efficiency of snow (Sanei et al., 2010; Faïn et al., 2011).

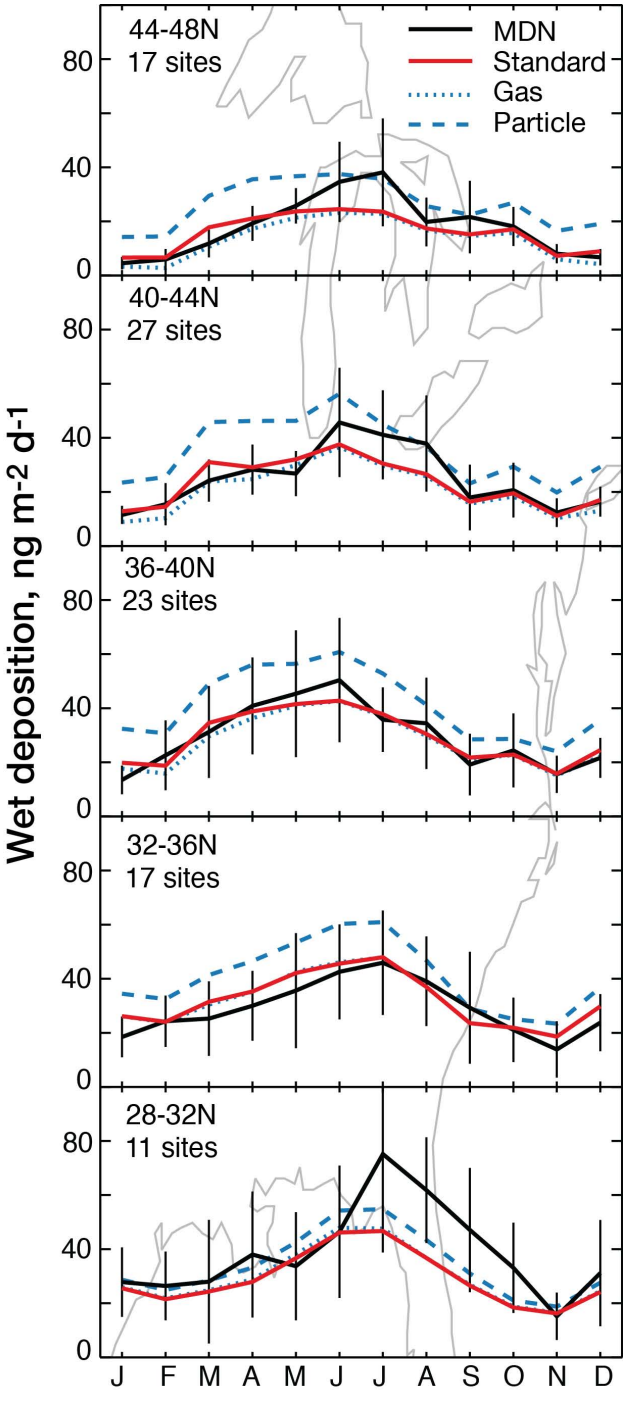


**Fig. 7.** Seasonal variation of Hg wet deposition fluxes in the eastern US for different latitude bands. Values are monthly means for 2007–2009 in the observations (black) and in the model (red, blue). Observations from Fig. 6 are averaged over all sites in the latitude band that meet data density criteria described by Holmes et al. (2010). Model results are sampled at the same sites and are shown for the standard simulation (red) and for sensitivity simulations where all Hg(II) is assumed to deposit as a gas (blue dotted) or as particles (blue dashed). Standard deviations are calculated from monthly means for individual MDN sites and individual years.

## 6 Conclusions

We have used long-term measurements of RGM and PBM at five sites in North America to derive an empirical gas-particle Hg(II) partitioning coefficient as a function of $PM_{2.5}$ and temperature: $\log_{10}(K^{-1}) = (10\pm1)–(2500\pm300)/T$ where $K = (PBM/PM_{2.5})/RGM$, PBM and RGM are in common mixing ratio units, $PM_{2.5}$ is in $\mu g\,m^{-3}$, and $T$ is in K.

Implementation of this Hg(II) gas-particle partitioning in the global 3-D GEOS-Chem Hg model yields Hg(II) fractions in the particle phase ranging from more than 90 % in cold air masses with high aerosol burdens to less than 10 % in warm air with low aerosol. Relative to a model simulation assuming all Hg(II) to be in the gas phase, Hg(II) deposition is increased at high latitudes because particulate Hg is more efficiently scavenged by snow, and decreased at subtropical latitudes because particulate Hg is less efficiently dry deposited.

The resulting GEOS-Chem simulation was evaluated with RGM and PBM observations as well as wet deposition fluxes of Hg over the US. Besides Hg(II) gas-particle partitioning, our model includes improvements to the washout algorithm and a change in the Hg(0):Hg(II):Hg(p) emission speciation for fossil fuel combustion from 50:40:10 to 86.5:9.9:3.6 (Y. Zhang et al., 2011). Adjusting the emission speciation in this manner greatly improves the simulation of RGM and PBM at North American sites. Little is known about the chemical or physical nature of primary Hg(p) included in current anthropogenic emission inventories. Here we assume that Hg(p) is emitted as Hg(II) and thus available for gas-particle partitioning. Previous versions of GEOS-Chem have assumed Hg(p) to be chemically inert but we find that this would cause an overestimate of PBM at North American sites.

We compared model results to seasonal observations of Hg(0), RGM, and PBM at the five North American surface sites used to construct the $K(T)$ parameterization. Observations in Reno and Milwaukee show particularly large summertime RGM that we attribute to subsidence of free tropospheric air (Reno) and regional anthropogenic sources (Milwaukee). Observations in rural New Hampshire (Thompson Farm) and Ontario (Experimental Lakes Area) show spring maxima in RGM and PBM that we attribute to UT/LS influence. These maxima are correlated in the model with cosmogenic $^7$Be, suggesting that $^7$Be measurements would be of value to separate global and local contributions in RGM and PBM observations.

Compared to the previous version of GEOS-Chem (Holmes et al., 2010), our model shows an improved ability to reproduce the observed spatial distribution of MDN annual Hg wet deposition fluxes over the US. Holmes et al. (2010) had found that implementing Br as an Hg(0) oxidant degraded the model's skill at simulating the MDN data relative to the older model version (Selin et al., 2007; Selin and Jacob, 2008) with oxidation by OH and $O_3$. Our improved simulation of the MDN data (using Br as the Hg(0) oxidant) largely reflects improvements in the washout algorithm. We still underestimate MDN wet deposition in Florida. The observed wintertime minimum in Hg deposition in the MDN data is attributed to inefficient snow scavenging of gaseous Hg(II).

## Appendix A

### GEOS-Chem algorithm for washout of soluble gases by rain

Below-cloud scavenging (washout) of gases by rain in GEOS-Chem is determined by Henry's law equilibrium but can also be limited by mass transfer for highly soluble gases (Levine and Schwartz, 1982). The fraction $F$ of gas scavenged from a grid box by washout over a time step $\Delta t$ as determined by Henry's law equilibrium is

$$F = f\frac{K^* L_p RT}{1 + K^* L_p RT} \tag{A1}$$

Here $f$ is the areal fraction of the grid box experiencing precipitation, $K^*$ is the effective Henry's law constant ($M\,atm^{-1}$) including any dissociation and complexation equilibria in the aqueous phase, $R$ is the universal gas constant, $T$ is temperature, and $L_p$ is the time-integrated rainwater content in the precipitating fraction of the grid box

$$L_p = \frac{P\Delta t}{f\Delta Z} \tag{A2}$$

where $P$ ($cm^3$ water $cm^{-2}$ surface $s^{-1}$) is the grid-averaged precipitation flux through the bottom of the grid box and $\Delta Z$ (cm) is the grid box thickness. For highly soluble gases, $F$ may be limited by molecular diffusion to the raindrops. On the basis of the detailed mass transfer calculations by Levine and Schwartz (1982) for diffusion-limited uptake of $HNO_3$, a maximum value $F_{max}$ for $F$ is derived as

$$F_{max} = f[1 - \exp(-k'\frac{P}{f}\Delta t)] \tag{A3}$$

where $k'$ ($cm^{-1}$) is a washout rate constant ($k' = 1\,cm^{-1}$; Table 2 of Levine and Schwartz, 1982).

GEOS-Chem computes $F$ and $F_{max}$ locally for every precipitating grid box and time step. If $F \le F_{max}$, we assume that washout is limited by Henry's law and the change in mass $\Delta m$ of the soluble gas due to washout over $\Delta t$ is then computed as

$$\Delta m = -Fm + m_T(1 - \frac{F}{f}) \tag{A4}$$

where $m$ is the mass of the gas in the grid box and $m_T$ is the cumulative mass of gas scavenged via precipitation from above and entering the top of the grid box over $\Delta t$ and over

the grid box fraction $f$. Equation (A4) allows for partial re-evaporation of the mass scavenged from above. If $F > F_{\max}$, we assume that washout is limited by mass transfer as given by Eq. (A3) and $\Delta m$ is then computed as

$$\Delta m = -F_{\max} m + \beta \alpha m_T \quad \text{(A5)}$$

where $\alpha$ is the fraction of precipitation falling through the top of the gridbox that evaporates within the gridbox and $\beta$ is the fraction of this re-evaporation that involves total evaporation of raindrops (which releases the gas to the gridbox) rather than partial shrinkage (which does not). We assume $\beta = 0.5$ for $\alpha < 1$ and $\beta = 1$ for $\alpha = 1$ (Liu et al., 2001).

Because of a coding error in GEOS-Chem, the algorithm described above was incorrectly executed in previous model versions so that washout of highly soluble gases ($F > F_{\max}$) was underestimated except for $HNO_3$ (which was correct). This affected the scavenging of gaseous Hg(II), for which a Henry's law constant of $1.4 \times 10^6$ M atm$^{-1}$ is assumed based on laboratory data for $HgCl_2$ (Lindqvist and Rodhe, 1985). Correcting the error, as done here in the standard simulation, decreases the lifetime of tropospheric gaseous Hg(II) against wet deposition from 104 days to 46 days.

*Acknowledgements.* This work was funded by the NSF Atmospheric Chemistry Program and by AMS and NSF Graduate Fellowships to HMA. HMA would like to thank Lee T. Murray for helpful instruction on using the GEOS-Chem Be-Pb-Rn simulation and Leonard Levin for helpful discussion. Funding for the collection of data at the Experimental Lakes Area was provided by NSERC, Environment Canada and Manitoba Hydro. We kindly thank the two anonymous reviewers for their comments and for helping improve this manuscript.

Edited by: J. H. Seinfeld

## References

Alegría, N., Herranz, M., Idoeta, R., and Legarda, F.: Study of Be-7 activity concentration in the air of northern Spain, J. Radioanal. Nucl. Chem., 286, 347–351, doi:10.1007/s10967-010-0710-6, 2010.

AMAP/UNEP: Technical Background Report to the Global Atmospheric Mercury Assessment. Arctic Monitoring and Assessment Programme/UNEP Chemical Branch. 159 pp., 2008.

Arnott, W., Gyawali, M., and Arnold, I.: Aerosol extinction and single scattering albedo downwind of the summer 2008 California wildfires measured with photoacoustic spectrometers and sunphotometers from 355 nm to 1047 nm. Eos, 89, AGU Fall Meeting Supplement, Abstract A11D-0169, 2008.

Balkanski, Y. J., Jacob, D. J., and Gardner, G. M.: Transport and residence times of tropospheric aerosols inferred from a global three-dimensional simulation of Pb-210, J. Geophys. Res., 98, 20573–20586, 1993.

Bergan, T. and Rodhe, H.: Oxidation of elemental mercury in the atmosphere; constraints imposed by global scale modeling, J. Atmos. Chem., 40, 191–212, 2001.

Bullock, O. R. and Brehme, K. A.: Atmospheric mercury simulation using the CMAQ model: Formulation description and analysis of wet deposition results, Atmos. Environ., 36, 2135–2146, 2002.

Calvert, J. G., and Lindberg, S. E.: Mechanisms of mercury removal by O-3 and OH in the atmosphere, Atmos. Environ., 39, 3355–3367, doi:10.1016/j.atmosenv.2005.01.055, 2005.

Chung, S. H. and Seinfeld, J. H.: Global distribution and climate forcing of carbonaceous aerosols, J. Geophys. Res., 107, 4407, doi:10.1029/2001JD001397, 2002.

Clarkson, T. W. and Magos, L.: The toxicology of mercury and its chemical compounds, Crit. Rev. Toxic. , 36, 609–662, 2006.

Clever, H. L., Johnson, S. A., and Derrick, M. E.: The solubility of mercury and some sparingly soluble mercury salts in water and aqueous-electrolyte solutions, J. Phys. Chem. Ref. Data, 14, 631–681, 1985.

Dastoor, A. P. and Larocque, Y.: Global circulation of atmospheric mercury: A modeling study, Atmos. Environ., 38, 147–161, doi:10.1016/j.atmosenv.2003.08.037, 2004.

Edgerton, E. S., Hartsell, B. E., and Jansen, J. J.: Mercury speciation in coal-fired power plant plumes observed at three surface sites in the southeastern US, Environ. Sci. Technol., 40, 4563–4570, doi:10.1021/es0515607, 2006.

Engle, M. A., Tate, M. T., Krabbenhoft, D. P., Schauer, J. J., Kolker, A., Shanley, J. B., and Bothner, M. H.: Comparison of atmospheric mercury speciation and deposition at nine sites across central and eastern North America, J. Geophys. Res., 115, D18306, doi:10.1029/2010jd014064, 2010.

Faïn, X., Obrist, D., Hallar, A. G., McCubbin, I., and Rahn, T.: High levels of reactive gaseous mercury observed at a high elevation research laboratory in the Rocky Mountains, Atmos. Chem. Phys., 9, 8049–8060, doi:10.5194/acp-9-8049-2009, 2009.

Faïn, X., Obrist, D., Pierce, A., Barth, C., Gustin, M. S., and Boyle, D. P.: Whole-watershed mercury balance at Sagehen Creek, Sierra Nevada, CA, Geochim. Cosmochim. Acta, 75, 2379–2392, doi:10.1016/j.gca.2011.01.041, 2011.

Finley, B. D., Swartzendruber, P. C., and Jaffe, D. A.: Particulate mercury emissions in regional wildfire plumes observed at the Mount Bachelor Observatory, Atmos. Environ., 43, 6074–6083, doi:10.1016/j.atmosenv.2009.08.046, 2009.

Friedli, H. R., Radke, L. F., Lu, J. Y., Banic, C. M., Leaitch, W. R., and MacPherson, J. I.: Mercury emissions from burning of biomass from temperate North American forests: Laboratory and airborne measurements, Atmos. Environ., 37, 253–267, doi:10.1016/s1352-2310(02)00819-1, 2003a.

Friedli, H. R., Radke, L. F., Prescott, R., Hobbs, P. V., and Sinha, P.: Mercury emissions from the August 2001 wildfires in Washington State and an agricultural waste fire in Oregon and atmospheric mercury budget estimates, Glob. Biogeochem. Cy, 17, 1039, doi:10.1029/2002GB001972, 2003b.

Galarneau, E., Bidleman, T. F., and Blanchard, P.: Seasonality and interspecies differences in particle/gas partitioning of PAHs observed by the Integrated Atmospheric Deposition Network (IADN), Atmos. Environ., 40, 182–197, doi:10.1016/j.atmosenv.2005.09.034, 2006.

Graydon, J. A., Louis, V. L. S., Hintelmann, H., Lindberg, S. E., Sandilands, K. A., Rudd, J. W. M., Kelly, C. A., Hall, B. D., and Mowat, L. D.: Long-term wet and dry deposition of total and methyl mercury in the remote boreal ecoregion of Canada,

Environ. Sci. Technol., 42, 8345–8351, doi:10.1021/es801056j, 2008.

Gustin, M. and Jaffe, D.: Reducing the uncertainty in measurement and understanding of mercury in the atmosphere, Environ. Sci. Technol., 44, 2222–2227, doi:10.1021/es902736k, 2010.

Hall, B.: The gas-phase oxidation of elemental mercury by ozone, Water Air Soil Pollut., 80, 301–315, doi:10.1007/bf01189680, 1995.

Hedgecock, I. M. and Pirrone, N.: Mercury and photochemistry in the marine boundary layer-modeling studies suggest the in situ production of reactive gas phase mercury, Atmos. Environ., 35, 3055–3062, doi:10.1016/s1352-2310(01)00109-1, 2001.

Holmes, C. D., Jacob, D. J., Mason, R. P., and Jaffe, D. A.: Sources and deposition of reactive gaseous mercury in the marine atmosphere, Atmos. Environ., 43, 2278–2285, doi:10.1016/j.atmosenv.2009.01.051, 2009.

Holmes, C. D., Jacob, D. J., Corbitt, E. S., Mao, J., Yang, X., Talbot, R., and Slemr, F.: Global atmospheric model for mercury including oxidation by bromine atoms, Atmos. Chem. Phys., 10, 12037–12057, doi:10.5194/acp-10-12037-2010, 2010.

Hynes, A., Donohoue, D., Goodsite, M., Hedgecock, I., Pirrone, N., and Mason, R.: Our current understanding of major chemical and physical processes affecting mercury dynamics in the atmosphere and at air-water/terrestrial interfaces, in: Mercury Fate and Transport in the Global Atmosphere, edited by: Pirrone, N. and Mason, R. P., chap. 14, Springer, 322–344, 2009.

Keeler, G., Glinsorn, G., and Pirrone, N.: Particulate mercury in the atmosphere – its significance, transport, transformation and sources, Water Air Soil Pollut., 80, 159–168, doi:10.1007/bf01189664, 1995.

Keeler, G. J., Gratz, L. E., and Al-Wali, K.: Long-term atmospheric mercury wet deposition at Underhill, Vermont, Ecotoxicology, 14, 71–83, doi:10.1007/s10646-004-6260-3, 2005.

Koch, D. M., Jacob, D. J., and Graustein, W. C.: Vertical transport of tropospheric aerosols as indicated by Be-7 and Pb-210 in a chemical tracer model, J. Geophys. Res., 101, 18651–18666, doi:10.1029/96jd01176, 1996.

Kos, G., Ryzhkov, A., and Dastoor, A.: Analysis of uncertainties in measurements and mode for oxidised and particle-bound mercury, 10th International Conference on Mercury as a Global Pollutant, Halifax, Nova Scotia, Canada, 2011.

Lamborg, C. H., Fitzgerald, W. F., Vandal, G. M., and Rolfhus, K. R.: Atmospheric mercury in northern Wisconsin – sources and species, Water Air Soil Pollut., 80, 189–198, doi:10.1007/bf01189667, 1995.

Landis, M. S., Stevens, R. K., Schaedlich, F., and Prestbo, E. M.: Development and characterization of an annular denuder methodology for the measurement of divalent inorganic reactive gaseous mercury in ambient air, Environ. Sci. Technol., 36, 3000–3009, doi:10.1021/es015887t, 2002.

Levine, S. Z. and Schwartz, S. E.: In-cloud and below-cloud scavenging of nitric acid vapor, Atmos. Environ., 16, 1725–1734, 1982.

Lin, C. J., Pongprueksa, P., Lindberg, S. E., Pehkonen, S. O., Byun, D., and Jang, C.: Scientific uncertainties in atmospheric mercury models I: Model science evaluation, Atmos. Environ., 40, 2911–2928, doi:10.1016/j.atmosenv.2006.01.009, 2006.

Lindberg, S. E. and Stratton, W. J.: Atmospheric mercury speciation: Concentrations and behavior of reactive gaseous mercury in ambient air, Environ. Sci. Technol., 32, 49–57, doi:10.1021/es970546u, 1998.

Lindqvist, O. and Rodhe, H.: Atmospheric mercury - a review, Tellus B-Chem. Phys. Meteorol., 37, 136–159, 1985.

Liu, H. Y., Jacob, D. J., Bey, I., and Yantosca, R. M.: Constraints from Pb-210 and Be-7 on wet deposition and transport in a global three-dimensional chemical tracer model driven by assimilated meteorological fields, J. Geophys. Res., 106, 12109–12128, doi:10.1029/2000jd900839, 2001.

Lohman, K., Seigneur, C., Edgerton, E., and Jansen, J.: Modeling mercury in power plant plumes, Environ. Sci. Technol., 40, 3848–3854, doi:10.1021/es051556v, 2006.

Lombard, M. A. S., Bryce, J. G., Mao, H., and Talbot, R.: Mercury deposition in southern New Hampshire, 2006–2009, Atmos. Chem. Phys., 11, 7657–7668, doi:10.5194/acp-11-7657-2011, 2011.

Lyman, S. N., Gustin, M. S., Prestbo, E. M., and Marsik, F. J.: Estimation of dry deposition of atmospheric mercury in Nevada by direct and indirect methods, Environ. Sci. Technol., 41, 1970–1976, doi:10.1021/es062323m, 2007.

Lyman, S. N., Gustin, M. S., Prestbo, E. M., Kilner, P. I., Edgerton, E., and Hartsell, B.: Testing and application of surrogate surfaces for understanding potential gaseous oxidized mercury dry deposition, Environ. Sci. Technol., 43, 6235–6241, doi:10.1021/es901192e, 2009.

Lyman, S. N. and Gustin, M. S.: Determinants of atmospheric mercury concentrations in Reno, Nevada, USA, Sci. Total Environ., 408, 431–438, doi:10.1016/j.scitotenv.2009.09.045, 2009.

Lyman, S. N., Jaffe, D. A., and Gustin, M. S.: Release of mercury halides from KCl denuders in the presence of ozone, Atmos. Chem. Phys., 10, 8197–8204, 10, http://www.atmos-chem-phys.net/10/8197/10/.5194/acp-10-8197-2010, 2010.

Lynam, M. M. and Keeler, G. J.: Artifacts associated with the measurement of particulate mercury in an urban environment: The influence of elevated ozone concentrations, Atmos. Environ., 39, 3081–3088, doi:10.1016/j.atmosenv.2005.01.036, 2005

Mahaffey, K. R., Clickner, R. P., and Bodurow, C. C.: Blood organic mercury and dietary mercury intake: National health and nutrition examination survey, 1999 and 2000, Environ. Health Persp., 112, 562–570, 2004.

Mahaffey, K. R., Clickner, R. P., and Jeffries, R. A.: Adult women's blood mercury concentrations vary regionally in the United States: Association with patterns of fish consumption (NHANES 1999–2004), Environ. Health Persp., 117, 47–53, 10.1289/ehp.11674, 2009.

Malcolm, E. G. and Keeler, G. J.: Evidence for a sampling artifact for particulate-phase mercury in the marine atmosphere, Atmos. Environ., 41, 3352–3359, doi:10.1016/j.atmosenv.2006.12.024, 2007.

Mao, H., Talbot, R., Hegarty, J., and Koermer, J.: Speciated mercury at marine, coastal, and inland sites in New England Part 2: Relationships with atmospheric physical parameters, Atmos. Chem. Phys. Discuss., 11, 28395–28443, doi:10.5194/acpd-11-28395-2011, 2011.

Mason, R. P. and Sheu, G. R.: Role of the ocean in the global mercury cycle, Global Biogeochem. Cy., 16, 1093, doi:10.1029/2001gb001440, 2002.

Mergler, D., Anderson, H. A., Chan, L. H. M., Mahaffey, K. R.,

Murray, M., Sakamoto, M., and Stern, A. H.: Methylmercury exposure and health effects in humans: A worldwide concern, Ambio, 36, 3–11, 2007.

Muramatsu, H., Yoshizawa, S., Abe, T., Ishii, T., Wada, M., Horiuchi, Y., and Kanekatsu, R.: Variation of Be-7 concentration in surface air at Nagano, Japan, J. Radioanal. Nucl. Chem., 275, 299–307, doi:10.1007/s10967-007-7056-8, 2008.

National Atmospheric Deposition Program: Mercury Deposition Network (MDN): A NADP Network, available online at: http://nadp.sws.uiuc.edu/MDN/, 2011.

Odum, J. R., Hoffmann, T., Bowman, F., Collins, D., Flagan, R. C., and Seinfeld, J. H.: Gas/particle partitioning and secondary organic aerosol yields, Environ. Sci. Technol., 30, 2580–2585, doi:10.1021/es950943, 1996.

Pacyna, E. G., Pacyna, J. M., Sundseth, K., Munthe, J., Kindbom, K., Wilson, S., Steenhuisen, F., and Maxson, P.: Global emission of mercury to the atmosphere from anthropogenic sources in 2005 and projections to 2020, Atmos. Environ., 44, 2487–2499, doi:10.1016/j.atmosenv.2009.06.009, 2010.

Pankow, J. F.: Review and comparative-analysis if the theories on partitioning between the gas and aerosol particulate phases in the atmosphere, Atmos. Environ., 21, 2275–2283, doi:10.1016/0004-6981(87)90363-5, 1987.

Pankow, J. F., Storey, J. M. E., and Yamasaki, H.: Effects of relative-humidity on gas-particle partitioning of semivolatile organic-compounds to urban particulate matter, Environ. Sci. Technol., 27, 2220–2226, doi:10.1021/es00047a032, 1993.

Pankow, J. F.: An absorption-model of the gas aerosol partitioning involved in the formation of secondary organic aerosol, Atmos. Environ., 28, 189–193, doi:10.1016/1352-2310(94)90094-9, 1994.

Petersen, G., Munthe, J., Pleijel, K., Bloxam, R., and Kumar, A. V.: A comprehensive Eulerian modeling framework for airborne mercury species: Development and testing of the tropospheric chemistry module (TCM), Atmos. Environ., 32, 829–843, doi:10.1016/s1352-2310(97)00049-6, 1998.

Petersen, G., Iverfeldt, A., and Munthe, J.: Atmospheric mercury species over central and northern Europe – model-calculations and comparison with observations from the Nordic Air and Precipitation Network for 1987 and 1988, Atmos. Environ., 29, 47–67, doi:10.1016/1352-2310(94)00223-8, 1995.

Poissant, L., Pilote, M., Xu, X. H., Zhang, H., and Beauvais, C.: Atmospheric mercury speciation and deposition in the Bay St. Francois wetlands, J. Geophys. Res., 109, D11301, 10.1029/2003jd004364, 2004.

Pongprueksa, P., Lin, C. J., Lindberg, S. E., Jang, C., Braverman, T., Bullock, O. R., Ho, T. C., and Chu, H. W.: Scientific uncertainties in atmospheric mercury models III: Boundary and initial conditions, model grid resolution, and Hg(II) reduction mechanism, Atmos. Environ., 42, 1828–1845, doi:10.1016/j.atmosenv.2007.11.020, 2008.

Rutter, A. P. and Schauer, J. J.: The impact of aerosol composition on the particle to gas partitioning of reactive mercury, Environ. Sci. Technol., 41, 3934–3939, doi:10.1021/es062439i, 2007a.

Rutter, A. P. and Schauer, J. J.: The effect of temperature on the gas-particle partitioning of reactive mercury in atmospheric aerosols, Atmos. Environ., 41, 8647–8657, doi:10.1016/j.atmosenv.2007.07.024, 2007b.

Rutter, A. P., Hanford, K. L., Zwers, J. T., Perillo-Nicholas, A. L., Schauer, J. J., and Olson, M. L.: Evaluation of an offline method for the analysis of atmospheric reactive gaseous mercury and particulate mercury, J. Air Waste Manage. Assoc., 58, 377–383, 10.3155/1047-3289.58.3.377, 2008a.

Rutter, A. P., Schauer, J. J., Lough, G. C., Snyder, D. C., Kolb, C. J., Von Klooster, S., Rudolf, T., Manolopoulos, H., and Olson, M. L.: A comparison of speciated atmospheric mercury at an urban center and an upwind rural location, J. Environ. Monit., 10, 102–108, doi:10.1039/b710247j, 2008b.

Sanei, H., Outridge, P. M., Goodarzi, F., Wang, F., Armstrong, D., Warren, K., and Fishback, L.: Wet deposition mercury fluxes in the Canadian sub-Arctic and southern Alberta, measured using an automated precipitation collector adapted to cold regions, Atmos. Environ., 44, 1672–1681, doi:10.1016/j.atmosenv.2010.01.030, 2010.

Scheuhammer, A. M., Meyer, M. W., Sandheinrich, M. B., and Murray, M. W.: Effects of environmental methylmercury on the health of wild birds, mammals, and fish, Ambio, 36, 12–18, doi:10.1579/0044-7447(2007)36[12:eoemot]2.0.co;2, 2007.

Schroeder, W. H. and Munthe, J.: Atmospheric mercury – an overview, Atmos. Environ., 32, 809–822, doi:10.1016/s1352-2310(97)00293-8, 1998.

Seigneur, C., Abeck, H., Chia, G., Reinhard, M., Bloom, N. S., Prestbo, E., and Saxena, P.: Mercury adsorption to elemental carbon (soot) particles and atmospheric particulate matter, Atmos. Environ., 32, 2649–2657, doi:10.1016/s1352-2310(97)00415-9, 1998.

Seigneur, C., Karamchandani, P., Lohman, K., Vijayaraghavan, K., and Shia, R. L.: Multiscale modeling of the atmospheric fate and transport of mercury, J. Geophys. Res., 106, 27795–27809, doi:10.1029/2000jd000273, 2001.

Seigneur, C., Karamchandani, P., Vijayaraghavan, K., Lohman, K., Shia, R. L., and Levin, L.: On the effect of spatial resolution on atmospheric mercury modeling, Sci. Total Environ., 304, 73–81, doi:10.1016/s0048-9697(02)00558-2, 2003.

Seigneur, C., Vijayaraghavan, K., and Lohman, K.: Atmospheric mercury chemistry: Sensitivity of global model simulations to chemical reactions, J. Geophys. Res., 111, D22306, doi:10.1029/2005jd006780, 2006.

Seinfeld, J. H. and Pandis, S. N.: Atmospheric chemistry and physics: From air pollution to climate change, 2nd ed., John Wiley & Sons, Inc., 1203 pp., 2006.

Selin, N. E., Jacob, D. J., Park, R. J., Yantosca, R. M., Strode, S., Jaegle, L., and Jaffe, D.: Chemical cycling and deposition of atmospheric mercury: Global constraints from observations, J. Geophys. Res., 112, D02308, doi:10.1029/2006jd007450, 2007.

Selin, N. E. and Jacob, D. J.: Seasonal and spatial patterns of mercury wet deposition in the United States: Constraints on the contribution from North American anthropogenic sources, Atmos. Environ., 42, 5193–5204, 2008.

Selin, N. E., Jacob, D. J., Yantosca, R. M., Strode, S., Jaegle, L., and Sunderland, E. M.: Global 3-D land-ocean-atmosphere model for mercury: Present-day versus preindustrial cycles and anthropogenic enrichment factors for deposition, Global Biogeochem. Cycles, 22, GB3099, doi:10.1029/2008gb003282, 2008.

Sigler, J. M., Mao, H., and Talbot, R.: Gaseous elemental and reactive mercury in southern New Hampshire, Atmos. Chem. Phys., 9, 1929–1942, doi:10.5194/acp-9-1929-2009, 2009.

Skov, H., Brooks, S. B., Goodsite, M. E., Lindberg, S. E., Mey-

ers, T. P., Landis, M. S., Larsen, M. R. B., Jensen, B., McConville, G., and Christensen, J.: Fluxes of reactive gaseous mercury measured with a newly developed method using relaxed eddy accumulation, Atmos. Environ., 40, 5452–5463, doi:10.1016/j.atmosenv.2006.04.061, 2006.

Soerensen, A. L., Sunderland, E. M., Holmes, C. D., Jacob, D. J., Yantosca, R. M., Skov, H., Christensen, J. H., Strode, S. A., and Mason, R. P.: An improved global model for air-sea exchange of mercury: High concentrations over the North Atlantic, Environ. Sci. Technol., 44, 8574–8580, doi:10.1021/es102032g, 2010.

Sommar, J., Gardfeldt, K., Stromberg, D., and Feng, X. B.: A kinetic study of the gas-phase reaction between the hydroxyl radical and atomic mercury, Atmos. Environ., 35, 3049–3054, doi:10.1016/s1352-2310(01)00108-x, 2001.

Subir, M., Ariya, P. A., and Dastoor, A. P.: A review of uncertainties in atmospheric modeling of mercury chemistry I. Uncertainties in existing kinetic parameters - fundamental limitations and the importance of heterogeneous chemistry, Atmos. Environ., 45, 5664–5676, doi:10.1016/j.atmosenv.2011.04.046, 2011.

Sunderland, E. M., and Mason, R. P.: Human impacts on open ocean mercury concentrations, Global Biogeochem. Cy., 21, GB4022, 10.1029/2006GB002876, 2007.

Swartzendruber, P. C., Jaffe, D. A., Prestbo, E. M., Weiss-Penzias, P., Selin, N. E., Park, R., Jacob, D. J., Strode, S., and Jaegle, L.: Observations of reactive gaseous mercury in the free troposphere at the Mount Bachelor Observatory, J. Geophys. Res., 111, D24302, doi:10.1029/2006jd007415, 2006.

Talbot, R., Mao, H., Feddersen, D., Smith, M., Kim, S. Y., Sive, B. C., Haase, K., Ambrose, J., Zhou, Y., and Russo, R.: Comparison of particulate mercury measured with manual and automated methods, Atmosphere, 2, 1–20, doi:10.3390/atmos2010001, 2011.

ter Schure, A., Caffrey, J., Gustin, M. S., Holmes, C. D., Hynes, A., Landing, B., Landis, M. S., Laudel, D., Levin, L., Nair, U., Jansen, J., Ryan, J., Walters, J., Schauer, J. J., Volkamer, R., Waters, D., and Weiss, P.: An integrated approach to assess elevated mercury wet deposition and concentrations in the southeastern United States, 10th International Conference on Mercury as a Global Pollutant, Halifax, Nova Scotia, Canada, 2011.

Vijayaraghavan, K., Karamchandani, P., Seigneur, C., Balmori, R., and Chen, S. Y.: Plume-in-grid modeling of atmospheric mercury, J. Geophys. Res., 113, D24305, doi:10.1029/2008jd010580, 2008.

Wang, Q., Jacob, D. J., Fisher, J. A., Mao, J., Leibensperger, E. M., Carouge, C. C., Le Sager, P., Kondo, Y., Jimenez, J. L., Cubison, M. J., and Doherty, S. J.: Sources of carbonaceous aerosols and deposited black carbon in the Arctic in winter-spring: Implications for radiative forcing, Atmos. Chem. Phys., 11, 12453–12473, doi:10.5194/acp-11-12453-2011, 2011.

Wang, Y. H., Jacob, D. J., and Logan, J. A.: Global simulation of tropospheric O3-NOx-hydrocarbon chemistry 1. Model formulation, J. Geophys. Res., 103, 10713–10725, doi:10.1029/98jd00158, 1998.

Weiss-Penzias, P., Gustin, M. S., and Lyman, S. N.: Observations of speciated atmospheric mercury at three sites in Nevada: Evidence for a free tropospheric source of reactive gaseous mercury, J. Geophys. Res., 114, D14302, doi:10.1029/2008jd011607, 2009.

Weiss-Penzias, P. S., Gustin, M. S., and Lyman, S. N.: Sources of gaseous oxidized mercury and mercury dry deposition at two southeastern US sites, Atmos. Environ., 45, 4569–4579, doi:10.1016/j.atmosenv.2011.05.069, 2011.

Wesely, M. L.: Parameterization of surface resistances to gaseous dry deposition in regional-scale numerical-models, Atmos. Environ., 23, 1293–1304, doi:10.1016/0004-6981(89)90153-4, 1989.

Yamasaki, H., Kuwata, K., and Miyamoto, H.: Effects of ambient temperature on aspects of airborne polycyclic aromatic hydrocarbons, Environ. Sci. Technol., 16, 189–194, doi:10.1021/es00098a003, 1982.

Yoshimori, M.: Beryllium 7 radionucleide as a tracer of vertical air mass transport in the troposphere, Atmos. Remote Sens., 828–832, 2005.

Zhang, L., Jacob, D. J., Downey, N. V., Wood, D. A., Blewitt, D., Carouge, C. C., van Donkelaar, A., Jones, D. B. A., Murray, L. T., and Wang, Y.: Improved estimate of the policy-relevant background ozone in the United States using the GEOS-Chem global model with $1/2^\circ \times 2/3^\circ$ horizontal resolution over North America, Atmos. Environ., 45, 6769–6776, 2011a.

Zhang, L. Jacob, D. J., Knipping, E. M., Kumar, N., Munger, J. W., Carouge, C. C., van Donkelaar, A., Wang, Y., and D. Chen: Nitrogen deposition to the United States: distribution, sources, and processes, Atmos. Chem. Phys., submitted, 2011b.

Zhang, Y., Jaeglé, L., van Donkelaar, A., Martin, R. V., Holmes, C. D., Amos, H. M., Wang, Q., Jacob, D. J., Talbot, R., Artz, R., Holson, T. M., Felton, D., Miller, E. K., Perry, K. D., Schmeltz, D., Steffen, A., and Tordon, R.: Nested-grid simulation of mercury over North America, Atmos. Chem. Phys., submitted, 2011.